

# Efficient probabilistic methods for real-time fatigue damage prognosis

Yibing Xiang and Yongming Liu

*Department of Civil & Environment Engineering, Clarkson University, Potsdam, NY 13699-5710, USA*

*xiangyi@clarkson.edu*

*yliu@clarkson.edu*

## ABSTRACT

A general probabilistic fatigue crack growth prediction methodology for accurate and efficient damage prognosis is proposed in this paper. This methodology consists two major parts. First, the realistic random loading is transformed to an equivalent constant amplitude loading process based on a recently developed mechanism model. This transformation avoids the cycle-by-cycle calculation of fatigue crack growth under variable amplitude loading. Following this, an inverse first-order reliability method (IFORM) is used to evaluate the fatigue crack growth at an arbitrary reliability level. Inverse FORM method does not require a large number of function evaluations compared to the direct Monte Carlo simulation. Computational cost is significantly reduced and the proposed method is very suitable for real-time damage prognosis. Numerical examples are used to demonstrate the proposed method. Various experimental data under variable amplitude loading are collected and model predictions are compared with experimental data for model validation.\*

## 1 INTRODUCTION

Fatigue failure is one of most common failure modes for structures or components, e.g. aircrafts and rotorcrafts (S. K. Bhaumik, M. Sujata & M. A. Venkataswamy, 2008). The structures experience different load spectrums during the entire fatigue life. The applied fatigue cyclic loading on structures (S.

Pommier, 2003) is stochastic in nature, which changes the stress amplitude and stress ratio throughout the entire life of the structure. One big challenge in fatigue crack growth prediction is the proper inclusion of random loading history effects, because different loading sequences may induce different load-interaction effects (S. Mikheevskiy & G. Glinka, 2009). It may accelerate (underload) or decelerate (overload) the fatigue crack growth. During the last few decades, many studies have been performed to investigate the retardation of crack growth caused by single or multiple overloads (D. M. Corbly & P. F. Packman, 1973; J. R. Mohanty, B. B. Verma & P. K. Ray, 2009; K. T. Venkateswara Rao & R. O. Ritchie, 1988). Different models have been developed: yield zone models (O. E. Wheeler, 1972; E. R. Willenborg J, Wood RA, 1971), crack closure models (W. Elber, 1971; A. U. d. Koning, 1981; J. C. Newman, 1981; A. Ray, 2000), strip yield models (v. d. L. H. de Koning AU, 1981; J. C. Newman, 1981; A. Ray, 2000), and two-parameter approach (A. H. Noroozi, G. Glinka & S. Lambert, 2007; A. H. Noroozi, G. Glinka & S. Lambert, 2008). These models focus on different explanations of loading interaction effect and used different types of variable block loading for model validation. Realistic random loading cases and the statistical description of loading interaction effects have not been fully investigated in the past. Due to the complicated and nonlinear nature of random loading interaction, a cycle-by-cycle simulation is required for each different loading history and is computationally expensive for probabilistic analysis, which usually requires a large number of Monte Carlo simulations. In view of this, the objective of this paper is to develop an efficient probabilistic model for fatigue crack growth prediction, which is based on the statistical description of the applied random loading. The key idea is to derive an equivalent stress level based on the statistical description of the random loading, such as the probabilistic distribution of applied stress range and stress ratio. Then, the variable amplitude loading crack

\* This is an open-access article distributed under the terms of the Creative Commons Attribution 3.0 United States License, which permits unrestricted use, distribution, and reproduction in any medium, provided the original author and source are credited.

growth problem is reduced to an equivalent constant amplitude crack growth problem, which greatly facilitates the integration for crack length prediction.

Fatigue reliability is a time-dependent reliability problem and different metrics can be used to describe the random nature of fatigue damage. One common approach is to calculate the reliability/failure probability at a specified life (Y. Liu & S. Mahadevan, 2007; Y. Liu & S. Mahadevan, 2009a; Y. Liu & S. Mahadevan, 2009b). This approach is very useful for engineering design against fatigue since the service life is usually given in design problems. Both simulation-based method and the FORM method can be used for this purpose (Y. Liu & S. Mahadevan, 2009a). Another approach is the probabilistic life prediction, i.e. the remaining life estimation at a specified reliability level. This measure is very useful for damage prognosis and condition-based maintenance and is the focus of the current study. Direct Monte Carlo simulation can be used for probabilistic fatigue prediction, but is time-consuming for large scale applications. Efficient methods for the probabilistic fatigue life prediction are the key objective of the proposed study and the inverse reliability method is proposed for this purpose. The inverse reliability methods have been developed and used for the reliability-based design optimization (RBDO) problem (A. Der Kiureghian, Y. Zhang & C.-C. Li, 1994). The RBDO problem calculates the design variables under a specified reliability level, which is similar to the probabilistic fatigue life prediction problem (i.e., calculate the life variable under a specified reliability level). This is the motivation in the current study to investigate the inverse reliability method for fatigue prognosis.

This paper is organized as follows. First, the proposed equivalent stress is derived for some special variable amplitude histories without considering the load interaction effect. Numerical examples are demonstrated to show the feasibility of the proposed equivalent stress level concept. Next, a small time scale fatigue crack growth model is briefly discussed and is used to obtain a correction term in the proposed equivalent stress level for load interaction effect. Following this, uncertainty quantification of material variability is performed, and an efficient numerical algorithm for probabilistic crack growth is implemented for iterative search in the inverse FORM calculation. Model predictions are compared with existing experimental data for model validation. Finally, some conclusions and future work are given based on the current investigation.

## 2 Equivalent stress level without load interaction

### 2.1 Basic concept of the equivalent stress level

There are several different fatigue crack growth models, such as Forman's model (N. E. Dowling, 2007), Nasgro model (NASA, 2000), EIFS-based fatigue crack growth model (Y. Liu & S. Mahadevan, 2009b), and two-parameter approach (A. H. Noroozi et al., 2007; A. H. Noroozi et al., 2008). Different models focus on different aspects and will give different predictions. A generic function of crack growth rate curve can be expressed as

$$da/dN = f(\Delta\sigma, R, a) \quad (1)$$

Where  $a$  and  $N$  are the crack length and the fatigue life respectively.  $\Delta\sigma$  is the stress range and  $R$  is the stress ratio. Eq. (1) can be reformulated as

$$dN = \frac{1}{f(\Delta\sigma, R, a)} da \quad (2)$$

For arbitrary fatigue cycle  $i$ , the increment of crack length can be obtained by integrating both sides of Eq. (2).

$$N_i = \int_{a_i}^{a_{i+1}} \frac{1}{f(\Delta\sigma_i, R_i, a)} da \quad (3)$$

where  $a_i$  is the crack size at the beginning of cycle  $i$  and  $a_{i+1}$  is the crack size at the beginning of cycle  $i+1$ . The total fatigue life  $N$  under arbitrary random loading history is the summation of  $N_i$  and can be written as

$$N_{total} = \sum_{i=0}^n N_i = \sum_{i=0}^n \int_{a_i}^{a_{i+1}} \frac{1}{f(\Delta\sigma_i, R_i, a)} da \quad (4)$$

where  $a_0$  is the initial crack size and  $a_n$  is crack length at fatigue cycle  $N$ .

The aim of this paper is to find an equivalent crack growth process under constant amplitude loading, which produces a similar crack length with that of the true random loading case. In this ideal crack growth process, the stress level is constant and is the proposed equivalent stress level (ESL). The equivalent stress level can be expressed as

$$N_{total} = \int_{a_0}^{a_{n+1}} \frac{1}{f(\Delta\sigma_{eq}, R_{eq}, a)} da \quad (5)$$

The equivalent stress level can be obtained by equating Eq. (4) and Eq. (5) as

$$\int_{a_0}^{a_{n+1}} \frac{1}{f(\Delta\sigma_{eq}, R_{eq}, a)} da = \sum_{i=0}^n \int_{a_i}^{a_{i+1}} \frac{1}{f(\Delta\sigma_i, R_i, a)} da \quad (6)$$

Eq. (6) is the proposed equivalent stress level calculation and it can be applied to different types of crack growth models. For any arbitrary functions of  $f()$ . The analytical solution is not apparent and discussions of some special cases are given below.

## 2.2 Special cases of equivalent stress level

The stress range, stress ratio and corresponding fatigue cycle are random variables in the probabilistic crack growth analysis under general variable amplitude loading conditions. Several special cases are discussed first.

### Case 1: fixed stress ratio

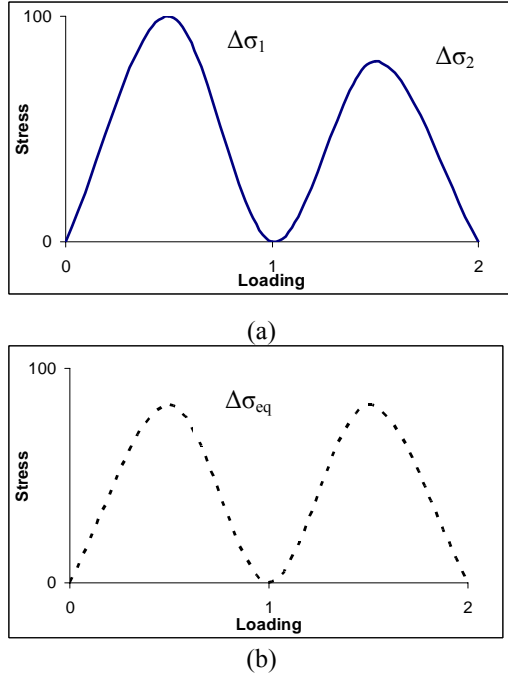


Fig.1 loading history: (a) variable amplitude loading, (b) equivalent loading

A simple case for fixed R ratio is illustrated first for a two different loading cycles, as shown in Fig. 1. The solid line represents an arbitrary variable amplitude loading (two cycles), and the dashed line represents the equivalent loading. Both the variable and constant loadings are under the same constant stress ratio. These two loadings have the same initial and final crack size. The fatigue crack growth caused by the equivalent stress range is the same as that caused by the two arbitrary loading cycles (Eq. (7)). The crack increments for the true loading history and the equivalent constant amplitude loading can be expressed as

$$\begin{aligned} N_{total} &= N_1 + N_2 \\ &= \int_{a_0}^{a_1} \frac{1}{f(\Delta\sigma_1, R, a)} da + \int_{a_1}^{a_2} \frac{1}{f(\Delta\sigma_2, R, a)} da \\ N_{total} &= \int_{a_0}^{a_2} \frac{1}{f(\Delta\sigma_{eq}, R, a)} da \end{aligned} \quad (7)$$

To further simplify the discussion, a modified Paris law is used to derive the analytical solution of the equivalent stress. The modified Paris law is expressed as

$$\frac{da}{dN} = C(\Delta K)^m = g(R)(\Delta K)^m \quad (8)$$

where  $C$  and  $m$  are the fitting parameters in the Paris law. Parameter  $C$  is expressed as a generic function of applied stress ratio to include the R ratio effect. For the case 1, the stress ratio is fixed and the  $C$  is a constant. Using Eq. (7) and the modified Paris law, the fatigue life  $N_i$  can be rewritten as

$$\begin{aligned} N_i &= \int_{\Delta K_i}^{\Delta K_{i+1}} \frac{1}{C(\Delta K)^m} d\left(\frac{\Delta K}{\Delta\sigma_i}\right)^2 \frac{1}{\pi} \\ &= \int_{\Delta K_i}^{\Delta K_{i+1}} \frac{2\Delta K}{C\Delta\sigma_i^2\pi(\Delta K)^m} d\Delta K \end{aligned} \quad (9)$$

where  $\Delta K_i = \Delta\sigma_i\sqrt{\pi a_i}$ . Eq. (9) can be rewritten as

$$\begin{aligned} N_i &= \frac{2}{C\Delta\sigma_i^2\pi} \left(\frac{R^{2-m}}{2-m}\right) \Big|_{\Delta K_i}^{\Delta K_{i+1}} \\ &= \frac{2\Delta\sigma_i^{2-m}\pi^{1-\frac{m}{2}}}{C\Delta\sigma_i^2\pi(2-m)} (a_{i+1}^{1-\frac{m}{2}} - a_i^{1-\frac{m}{2}}) \end{aligned} \quad (10)$$

In this case, only two loading cycles are considered. A relationship between the equivalent stress level and the variable loading can be developed combining Eq. (7) and Eq. (10) as

$$N_1\Delta\sigma_1^m + N_2\Delta\sigma_2^m = (N_1 + N_2)\Delta\sigma_{eq}^m \quad (11)$$

$$\Delta\sigma_{eq} = (p_1(\Delta\sigma_1)\Delta\sigma_1^m + p_2(\Delta\sigma_2)\Delta\sigma_2^m)^{\frac{1}{m}}$$

where  $p_1$  and  $p_2$  are the occurrence probability of these two variable loadings. This solution can be easily extended to infinity variable loading.

$$\Delta\sigma_{eq} = \left(\sum_1^n p_i(\Delta\sigma_i)\Delta\sigma_i^m\right)^{\frac{1}{m}} \quad (12)$$

### Case 2: fixed stress range

The above discussion is for variable loading cases with a fixed stress ratio. Another simple case is illustrated here, in which the stress range is fixed. As mentioned above, the parameter  $C$  in the modified Paris law is the a function of stress ratio (i.e.,  $C = g(R)$ ). Under a constant stress range, the fatigue life can be rewritten as:

$$\begin{aligned} N_i &= \frac{2}{g(R_i)\Delta\sigma^2\pi} \left(\frac{R^{2-m}}{2-m}\right) \Big|_{\Delta K_i}^{\Delta K_{i+1}} \\ &= \frac{g(0)}{g(R_i)} \frac{2\Delta\sigma^{2-m}\pi^{1-\frac{m}{2}}}{g(0)\Delta\sigma^2\pi(2-m)} (a_{i+1}^{1-\frac{m}{2}} - a_i^{1-\frac{m}{2}}) \end{aligned} \quad (13)$$

Firstly only two variable loading histories are considered. A relationship between equivalent stress and variable loading can be built:

$$\begin{aligned}
 N_1 \frac{g(R_1)}{g(0)} \Delta\sigma^m + N_2 \frac{g(R_2)}{g(0)} \Delta\sigma^m &= (N_1 + N_2) \Delta\sigma_{eq}^m \\
 \Delta\sigma_{eq} &= \left( \frac{N_1}{N_{total}} \frac{g(R_1)}{g(0)} + \frac{N_2}{N_{total}} \frac{g(R_2)}{g(0)} \right)^{\frac{1}{m}} \Delta\sigma \\
 &= (p_1(R_1) \frac{g(R_1)}{g(0)} + p_2(R_2) \frac{g(R_2)}{g(0)})^{\frac{1}{m}} \Delta\sigma
 \end{aligned} \quad (14)$$

where  $p_1$  and  $p_2$  are the occurrence probability of the two stress ratio. For more general cases of many fatigue cycles, the equivalent stress ratio can be described as

$$\begin{aligned}
 \Delta\sigma_{eq} &= \left( \sum_1^n \frac{N_i}{N_{total}} \frac{g(R_i)}{g(0)} \right)^{\frac{1}{m}} \Delta\sigma \\
 &= \left( \sum_1^n p_i(R_i) \frac{g(R_i)}{g(0)} \right)^{\frac{1}{m}} \Delta\sigma
 \end{aligned} \quad (15)$$

### Case 3: varying stress range and stress ratio

Above two special cases assume one of the applied loading parameters (e.g., stress range or stress ratio) is fixed. A general case is discussed here if both of them are random variables. A joint distribution of them is required for the derivation. In this case, the crack growth for any arbitrary cycle is determined by the following equation.

$$\begin{aligned}
 N_i &= \int_{\Delta a_i}^{\Delta a_{i+1}} \frac{1}{g(R_i) (\Delta\sigma_i \sqrt{\pi a})^m} da \\
 &= \frac{g(0)}{g(R_i)} \int_{\Delta a_i}^{\Delta a_{i+1}} \frac{1}{g(0) (\Delta\sigma_i \sqrt{\pi a} - \Delta K_{th})^m} da
 \end{aligned} \quad (16)$$

Following the same procedure, the general equivalent stress can be expressed as

$$\begin{aligned}
 \Delta\sigma_{eq} &= \left( \sum_1^n \frac{N_i}{N_{total}} \frac{g(R_i)}{g(0)} \Delta\sigma_i^m \right)^{\frac{1}{m}} \\
 &= \left( \sum_1^n p_i(R_i, \Delta\sigma_i) \frac{g(R_i)}{g(0)} \Delta\sigma_i^m \right)^{\frac{1}{m}}
 \end{aligned} \quad (17)$$

where  $p_i(R_i, \Delta\sigma_i)$  is the joint distribution of stress range and stress ratio. Eq. (17) is the generalized equivalent stress level expression without considering the loading interaction effect.

The proposed equivalent stress level in this Section is not a brand-new concept (N. E. Dowling, 2007). In the current study, the probabilistic distributions of stress range and stress ratio are integrated, which is easy for understanding and application.

### 3 Equivalent stress level considering load interaction

Section 2 discussed the equivalent stress level without considering load interaction.

It is well known that the ‘‘memory’’ effect (S. Mikheevskiy & G. Glinka, 2009) exists for fatigue

crack growth and coupling effect has to be considered. In this section, the previous developed equivalent stress model is extended to include the load interaction effect, such as the overload retardation and underload acceleration. The modification is based on a recently developed small time scale formulation of fatigue crack growth and a load interaction correction function.

#### 3.1 Small-Time-Scale (STS) model

A new small time scale model has been developed by Lu and Liu (Z. Lu & Y. Liu, 2010). This method is based on the incremental crack growth at any time instant within a cycle, and is different from the classical reversal-based fatigue analysis. This methodology is based on the interaction of forward and reverse plastic zone and has been validated under variable amplitude loadings, such as a combination of overload and underload. The small time scale method is briefly described below, and the detailed derivation can be found in the referred paper (Z. Lu & Y. Liu, 2010).

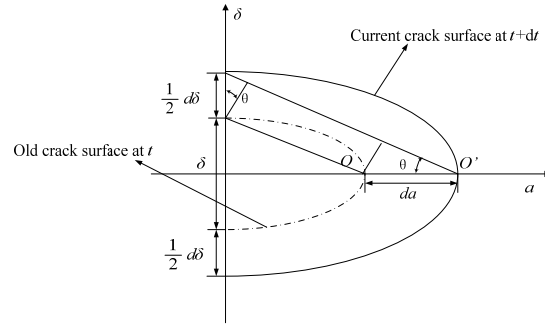


Fig. 2 Schematic representation of crack tip geometry

The developed incremental crack growth model is schematically shown in Fig. 2. The model is developed based on the geometric relationship between the crack tip opening displacement (CTOD) and the instantaneous crack growth kinetics. Considering the geometry of crack tips at two time instants ( $t$  and  $t + dt$ ), the relationship between the CTOD increment  $d\delta$  and the crack growth  $da$  can be expressed as

$$da = \frac{ctg\theta}{2} d\delta = Cd\delta \quad (18)$$

where  $C = \frac{ctg\theta}{2}$  and  $\theta$  is the crack tip opening angle (CTOA). It should be noted that Eq. (18) assumes the infinitesimal crack growth.

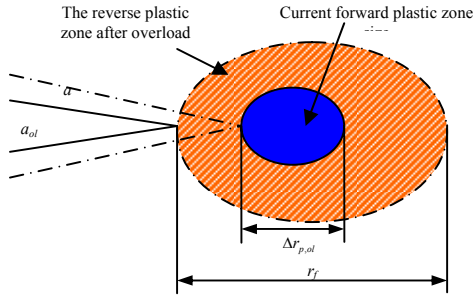


Fig.3 Illustration of forward and reverse plastic zone under variable amplitude loading

Crack growth prediction can be performed by directly integration of Eq. (18). The load interaction effect is modeled by the interaction of forward and reversed plastic zone model. A schematic explanation is shown in Fig. 3. The blue region and orange region represent the current forward plastic zone and the reverse plastic zone after overload. The limit state function is used to determine the crack growth regime during the time integration, i.e., shown as Eq. (19):

$$a_{ol} + \Delta r_{p,ol} = a + r_f \quad (19)$$

If overload exist in the history, a large reversed plastic zone occurs ahead of the crack tip and retards the crack growth.

### 3.2 Response function for load interaction

The key idea of this paper is the efficient calculation of probabilistic fatigue crack growth. As discussed in the Section 1, one big challenge for fatigue analysis for random loading case is how to handle the loading sequence effects. The traditional methods are using cycle-by-cycle-based simulation, which is computationally expensive for probabilistic analysis. To simplify the calculation, the developed small time scale model is used to find a response function of the applied random loading. In the current investigation, overload spectrums are used to demonstrate this response function construction. For overload spectrums, a correction term is added to handle the load interaction effect of the proposed equivalent stress level model. The equivalent stress level consider load interaction effect is defined as

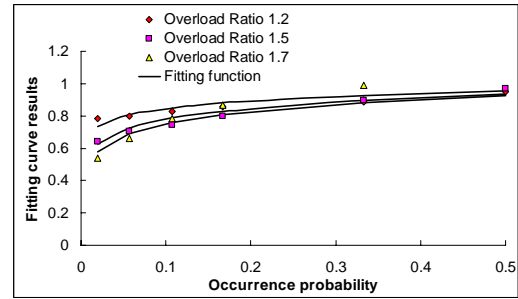
$$\Delta\sigma_{eq}^* = \eta\Delta\sigma_{eq} \quad (20)$$

where  $\Delta\sigma_{eq}^*$  is the equivalent stress level considering the load interaction effect and  $\Delta\sigma_{eq}$  is calculated using Eq. (17) without considering the load interaction term.  $\eta$  is the coefficient for the load interaction effect and is a function of the applied overload ratio  $R_{OL}$  and the occurrence probability  $P_{OL}$  of the overload cycles.

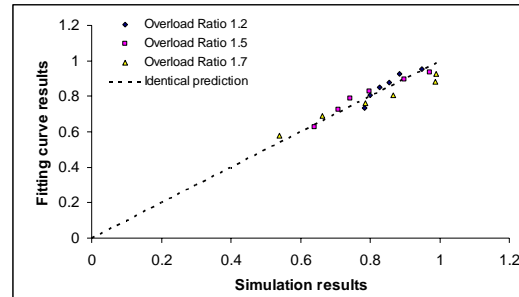
Because  $\eta$  does not have physical meaning, a method similar to DOE (design of experiment) combined with regression analysis is used to construct the response function. First,  $R_{OL}$  takes the value of 1.2, 1.5, and 1.7, respectively. At each value of  $R_{OL}$ , the  $P_{OL}$  takes the value of 0.020, 0.057, 0.107, 0.167, 0.333 and 0.5. In the current study, a nonlinear function as shown Eq. (21) is used to fit the simulation results.

$$\eta = k(R_{OL}, P_{OL}) = 1 + A \log(P_{OL})(R_{OL} - 1)^B \quad (21)$$

$k$  is a generic function and can be fitted using the numerical simulation results.  $A$  and  $B$  are fitting parameters and equals to 0.12 and 0.38, respectively. Fig. 4 (a) shows the fitting curve for three different overload ratios. A comparison of the fitted curve with simulation results is shown in Fig. 4 (b).



(a)



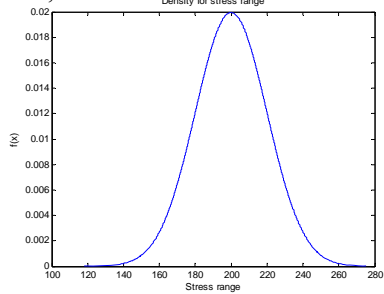
(b)

Fig.4 Comparison between fitting points with simulation results

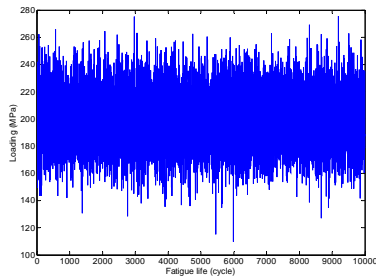
## 4 Numerical examples

A numerical example of fatigue crack growth is shown in Fig.5. The material is Al-7075 with an initial crack 1.27 mm. The probability density function (PDF) of stress range is shown in Fig. 5 (a), which follows a normal distribution with mean value 200 MPa and standard deviation 20 MPa. 10000 cycle random loading is shown in Fig.5 (b). The stress ratio is a constant equaling to -0.5. Using the fatigue model discussed in Section 2, the fatigue crack prediction has been performed using the equivalent stress level. A

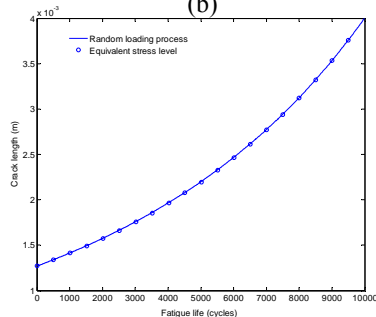
comparison has been shown in Fig. 5 (c). The dashed line is the fatigue crack growth curve under the true random loading history; and the solid line is the fatigue crack growth under equivalent stress range. Although some small discrepancy of fatigue crack growth curve can be seen, the same final crack size can be obtained.



(a)

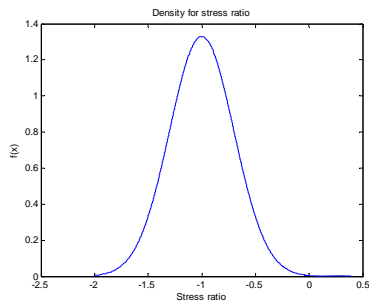


(b)

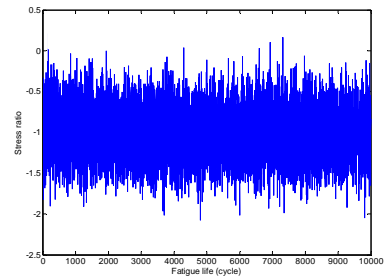


(c)

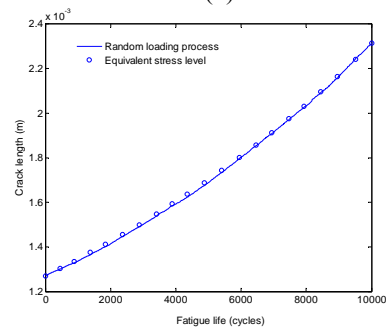
Fig.5 (a) distribution of the random loading, (b) a random loading history (fixed stress ratio), (c) Fatigue crack growth



(a)



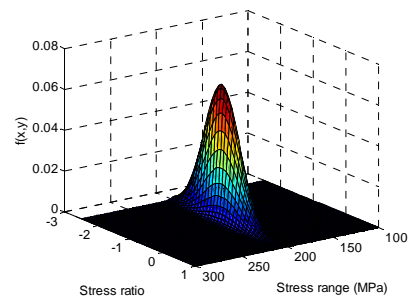
(b)



(c)

Fig.6 (a) distribution of the random loading, (b) a random loading history (fixed stress range), (c) Fatigue crack growth curves under random loading

A similar numerical example is performed for the fixed stress range case and is shown in Fig. 6. The loading follows a normal distribution as shown in Fig.6 (b). The history of 10000 cycle random loading is shown in Fig.6 (a). The random loading has the constant stress range equaling 150 MPa, but the stress ratios are random variables. The mean value and standard deviation of stress ratio are -1 and 0.3 respectively. Fatigue crack growth prediction has been done using equivalent stress amplitude. Good agreement of the final crack size can be observed in Fig. 6 (c).



(a)

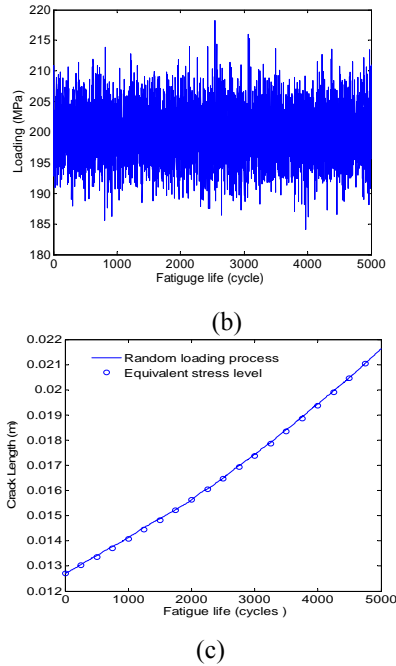


Fig.7 (a) Joint distribution of the random loading, (b) a random loading history, (c) Fatigue crack growth curves under random loading.

The last numerical example is applied to the general case where both stress range and stress ratio varies. A joint distribution (Gaussian) of stress range and stress ratio is shown in Fig. 7 (a). The mean value and standard deviation of stress range are 200 MPa and 20 MPa. The mean value and standard deviation of stress ratio are -1 and 0.3 respectively. The correlation coefficient between stress range and stress ratio is 0.1. The random 5000 loading history is shown in Fig. 7 (b). Fatigue crack prediction has been performed for this joint-distributed stress range and stress ratio. Satisfactory results are obtained

## 5 Inverse FORM method

Above discussion uses Monte Carlo simulation for probabilistic crack growth prediction. To further increase the computational efficiency, analytical reliability method is used to avoid large number of simulations in the direct MC method. A detailed comparison (cycle-by-cycle simulation, equivalent-stress-level with MC simulation, equivalent-stress-level with IFORM) has been done to demonstrate the efficiency of proposed method in Section 6. The Details of Inverse FORM method is shown below.

### 5.1 Inverse FORM methodology

The first-order reliability method is a widely used numerical technique to calculate the reliability or failure probability of various engineering problems (J.

Cheng & Q. S. Li, 2009; S. Thorndahl & P. Willems, 2008; D. V. Val, M. G. Stewart & R. E. Melchers, 1998). Many studies have been reported on static failure problems using the FORM method (L. Cizelj, B. Mavko & H. Riesch-Oppermann, 1994; T. H. Skaggs & D. A. Barry, 1996; S. Thorndahl & P. Willems, 2008). It has been applied to fatigue problems to calculate the time dependent reliability (T. Y. Kam, K. H. Chu & S. Y. Tsai, 1998; M. Liao, X. Xu & Q.-X. Yang, 1995; Y. Liu & S. Mahadevan, 2009a; Y. Xiang & Y. Liu, 2010 (accepted)). Unlike the FORM method (A. Haldar & S. Mahadevan, 2000; Y. Liu, Mahadevan, S, 2009), the inverse FORM method tries to solve the unknown parameters under a specified reliability or failure probability level, which is more suitable for probabilistic life prediction (i.e., remaining life estimation corresponding to a target reliability level).

Limit state function is required for the analytical reliability method. A generic limit state function is expressed as Eq. (22a) as a function of two sets of variables  $x$  and  $y$ .  $x$  is the random vector and represents material properties, loadings, and environmental factors, etc.  $y$  is the index variable vector, e.g., time and spatial coordinates. The limit state function is defined in the standard normal space in Eq. (22a) and the non-Gaussian variables will be discussed later. The limit state function definition is similar to the classical FORM method (A. Haldar & S. Mahadevan, 2000). The solution for the unknown parameters needs to satisfy the reliability constraints, which are described in Eq. (22b) and Eq. (22c).  $\beta$  is the reliability index, which is defined as the distance from origin to the most probable point (MPP) in the standard normal space. The failure probability  $P_f$  can be calculated using the cumulative distribution function (CDF)  $\Phi$  of the standard Gaussian distribution. Numerical search is required to find the optimum solution, which satisfies the limit state function (Eq. (22d)). Details of the general inverse FORM method and concept can be found in (A. Der Kiureghian et al., 1994).

$$\left\{ \begin{array}{l} (a) : g(x, y) = 0 \\ (b) : \|x\| = \beta_{target} \\ (c) : p_f = \Phi(-\beta_{target}) \\ (d) : \left\{ \begin{array}{l} (1) x + \frac{\|x\|}{\|\nabla_x g(x, y)\|} \nabla_x g(x, y) = 0 \quad (P_f < 50\%) \\ (2) x - \frac{\|x\|}{\|\nabla_x g(x, y)\|} \nabla_x g(x, y) = 0 \quad (P_f \geq 50\%) \end{array} \right. \end{array} \right. \quad (22)$$

The overall objective of the inverse FORM method is to find a non-negative function satisfying all constraint conditions specified in Eq. (22). Thus, the numerical search algorithm can be used to find the solutions of the unknown parameters. Numerical search algorithm is developed to iteratively solve the Eq. (22). The

search algorithm is expressed as Eq. (23) after  $k$  iterations.

$$\begin{cases} X_{k+1} \\ Y_{k+1} \end{cases} = \begin{cases} X_k \\ Y_k \end{cases} + d_k = \begin{cases} X_k \\ Y_k \end{cases} + (a_1 d_k^1 + a_2 d_k^2) \quad (23)$$

where  $d_k^1$  and  $d_k^2$  are the search directions corresponding to different merit functions and can be calculated using Eq. (24)

$$d_k^1 = \begin{bmatrix} \frac{[\nabla_x g(x,y) \cdot x] - g(x,y) \nabla_x g(x,y) - x}{\|\nabla_x g(x,y)\|^2} \nabla_x g(x,y) - x \\ 0 \end{bmatrix} \quad (24)$$

$$d_k^2 = \begin{bmatrix} -x - \beta_{target} \frac{\nabla_x g(x,y)}{\|\nabla_x g(x,y)\|} \\ \frac{[\nabla_x g(x,y) \cdot x] - g(x,y) + \beta_{target} \|\nabla_x g(x,y)\|}{\frac{\partial g(x,y)}{\partial y}} \end{bmatrix}$$

$a_1$  and  $a_2$  are the weight of function and can be calculated as

$$\begin{cases} a_1 = \frac{f^1(x)}{f^1(x) + f^2(x)} \\ a_2 = \frac{f^2(x)}{f^1(x) + f^2(x)} \end{cases} \quad (25)$$

Where:

$$f^1(x,y) = \frac{1}{2} k_1 \left\| x - \frac{[\nabla_x g(x,y) \cdot x]}{\|\nabla_x g(x,y)\|^2} \nabla_x g(x,y) \right\|^2 + \frac{1}{2} k_2 g(x,y)^2 \quad (26)$$

$$f^2(x,y) = \frac{1}{2} k_3 (\|x\| - \beta)^2$$

The convergence criterion for the numerical search algorithm is

$$\frac{(\|x_{k+1} - x_k\|^2 + \|y_{k+1} - y_k\|^2)^{\frac{1}{2}}}{(\|x_{k+1}\|^2 + \|y_{k+1}\|^2)^{\frac{1}{2}}} \leq \varepsilon \quad (27)$$

where  $\varepsilon$  is a small value and indicates that the relative difference between two numerical solutions is small enough to ensure the convergence. It is noted that the above derivation assumes the random variables are standard Gaussian variables. This paper uses the transformation method proposed by Rackwitz and Fiessler (R. a. F. Rackwitz, B, June 1976) to transform the non-Gaussian variables to their equivalent standard normal space before the use of the inverse method. The random variable transformation can be expressed as

$$\begin{cases} \Phi\left(\frac{x^* - \mu_X^N}{\sigma_X^N}\right) = F_X(x^*) \Rightarrow \mu_X^N = x^* - \Phi^{-1}[F_X(x^*)] \sigma_X^N \\ \frac{1}{\sigma_X^N} \phi\left(\frac{x^* - \mu_X^N}{\sigma_X^N}\right) = f_X(x^*) \Rightarrow \sigma_X^N = \frac{\phi(\Phi^{-1}[F_X(x^*)])}{f_X(x^*)} \end{cases} \quad (28)$$

where  $\Phi(\cdot)$  and  $F_X(x^*)$  are the cumulative distribution functions (CDF) of the standard normal and original

non-normal variables, respectively.  $\phi(\cdot)$  and  $f_X(x^*)$  are the probability density function (PDF) of the standard normal and original non-normal variables, respectively. This transformation works well for the fatigue problem in the current investigation since the distributions of random variables are not highly skewed. For highly skewed distribution, the transformation proposed by Rackwitz and Fiessler (R. a. F. Rackwitz, B, 1978) can be used instead.

In practical applications, the crack growth prediction with a certain confidence bound is usually required for risk assessment and decision making. If a confidence is specified, the crack growth corresponding to the specified confidence bounds can be calculated using the above mentioned inverse FORM method.

## 6 Probabilistic crack prediction and comparison with experimental data

Previous discussion did not include much more uncertainties than those of the material properties. Previous discussions do not include the uncertainties from material properties and only focused on the mean prediction. Monte Carlo simulation is used for probabilistic crack growth analysis and the fitting parameters in the constant amplitude loading testing are assumed to be random variables. These random variables represent the material uncertainties. The constant amplitude loading testing is shown in Fig. 8 for Al-7075 and fitted statistical distribution of material parameters is listed in Table 1. The experimental data are reported in (T. R. Porter, 1972). A summary of the properties of the specimens used for the collected experimental data are listed in Table 2.

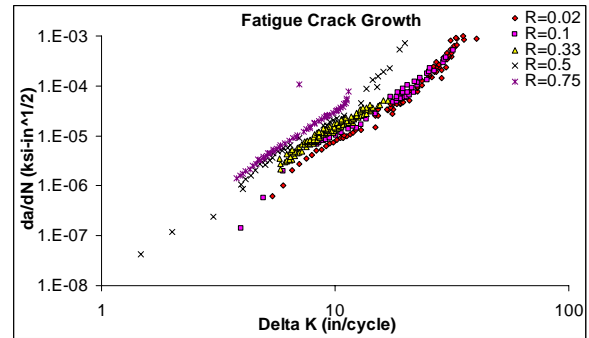


Fig. 8 Fatigue crack growth for Al-7075 under different stress ratios



Table 1 Stochastic coefficient of  $a$  and fatigue limit

Material	stress ratio	parameter	mean	std.
Al 7075-T6	0.03	$C$	7.72E-10	1.82E-10
		$K_c$	50	5
	0.05	$C$	7.96E-10	1.88E-10
		$K_c$	50	5

Table 2 Geometry and material properties of plate specimens

Specimen material	7075-T6
Ultimate strength $\sigma_u$ (MPa)	575
Yield strength $\sigma_y$ (MPa)	520
Modulus of elasticity $E$ (MPa)	69600
Plate width (mm)	305
Plate thickness (mm)	4.1
Ref.	(T. R. Porter, 1972)

Experimental data of Al 7075-T6 (T. R. Porter, 1972) under two blocks loading spectrum are used for model validation. A schematic illustration of the two blocks loading is shown in Fig. 9.  $p$  and  $n$  in Fig. 9 controls the number of cycles at the high amplitude and the low amplitude, respectively. Eight sets of experimental different block loadings (two constant and six variable amplitude loadings) are used for model validation and are plotted in Fig.9.  $p$  and  $n$  values for each spectrum loading are shown in the legend.

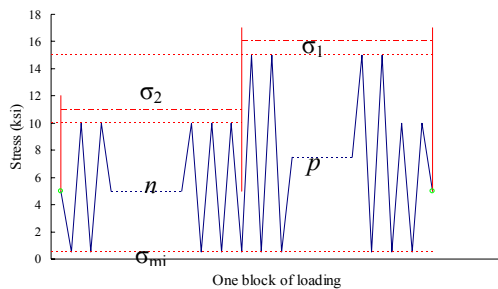
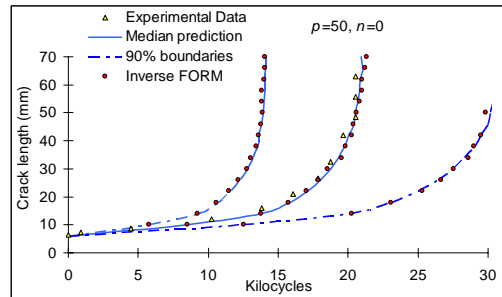


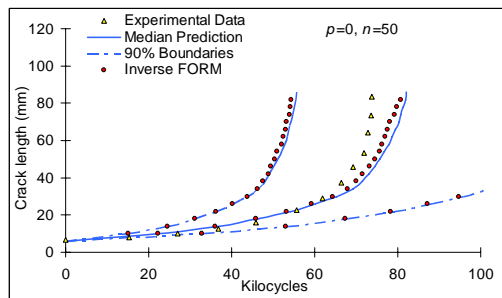
Fig. 9 Schematic illustration of the two blocks loading (T. R. Porter, 1972)

In Fig. 10, the fatigue crack growth prediction has been performed for Al-7075-T6. Both one thousand samples of Monte Carlo simulation (equivalent stress level) and Inverse FORM method are used to calculate the probabilistic fatigue crack distribution. In Fig. 10, the fatigue crack growth prediction results for Al-7075 have been shown for 2 constant amplitude loading cases ((a),(b)) and 6 variable amplitude loading cases ((c)~(h)). The triangles shown in Fig. 10 are the experimental data (T. R. Porter, 1972). The solid lines

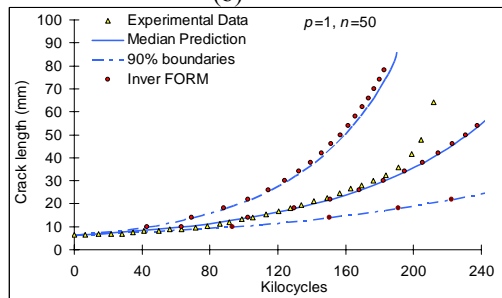
and the dashed lines represent median prediction of fatigue crack growth and 90% confidence bounds using Monte Carlo simulation, respectively. The dots shown in Fig. 10 are for the results of median and 90% confidence bounds using the inverse FORM method. It is shown that the inverse FORM results agree well with Monte-Carlo simulation for the median fatigue life prediction and 90% confidence bounds. Both methods capture the major trends of fatigue life curves and scatters.



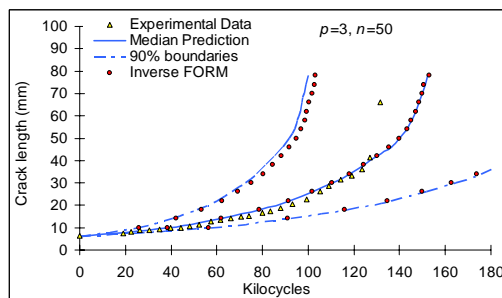
(a)



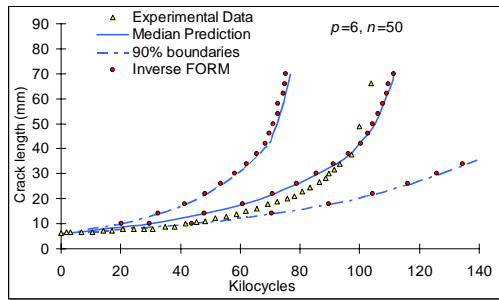
(b)



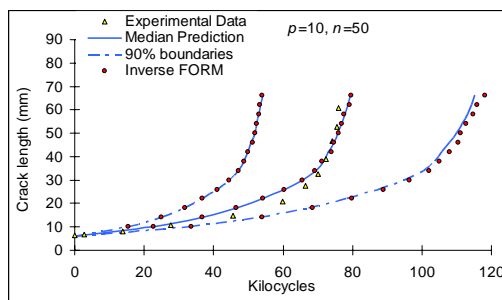
(c)



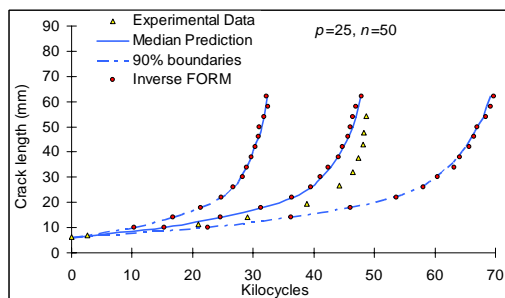
(d)



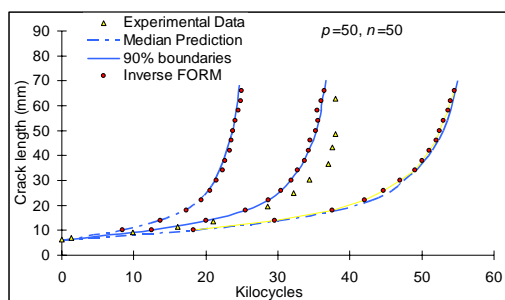
(e)



(f)



(g)



(h)

Fig. 10 Comparison of the predicted results with the experimental data of Al 7075-T6 under two block loading (T. R. Porter, 1972)

A very large scatter of fatigue crack prediction can be observed in Fig. 10. This is because large variance of the two input random variables. In the current study, the random variables are assumed to be independent and the correlation effects will be included in future study.

A summary of computation time using three different approaches are shown in the Table 3. The computations are performed using the same PC: dual core (intel 6600) with 4gb rams and windows 7 OS. MATLAB 2009b is the program used in the current study. For cycle-by-cycle simulation, the computation time for simulation single run is about 5 hours. 1000 sample cycle-by-cycle MC simulation is estimated. It can be easily observed that, the MC simulation using the equivalent stress level is much more efficient. It is shown that the most efficient one is the equivalent stress level concept with the inverse FORM. The computational time is several magnitudes less than both cycle-by-cycle and equivalent-stress-level-based MC simulation. Thus, the proposed method (equivalent stress level with inverse FORM) is very useful for real-time damage prognosis and is potentially initial damage tolerance design. It should be noted that a large number of MC simulation is required for very low failure probability (e.g., one million samples for 0.001% failure probability) to increase the simulation efficiency. In that case, the ratio of computational time of the proposed method and the direct MC will be even larger. Due to the extreme long computational time, direct MC simulations with a large number of simulation samples were not performed.

Table 3 Summary of computation time

Approach	Computation time
Cycle-by-cycle simulation (1000 sample MC simulation)	5000 hours (estimated)
Equivalent stress level (1000 sample MC simulation)	1 hours
Equivalent stress level (Inverse FORM)	50 seconds

## 7 Conclusion

In this paper, an efficient probabilistic methodology is proposed for fatigue crack growth prognosis. The proposed method simplifies the fatigue crack growth analysis under general random loadings and does not need cycle-by-cycle calculation. Analytical inverse FORM method avoids large number of simulations and further enhances the computational efficiency. The advantage makes it very suitable real-time damage prognosis and decision making. Extensive experimental data for Al-7075-T6 under two blocking loading spectrum are used to demonstrate the validation of the proposed methodology. Generally, the model

predictions agree with experimental observations well. Current study focused on two blocking loading spectrums. Future study is required to extend the proposed method to structural system applications under general random loadings. Online prognosis will be investigated based on the proposed methodology.

#### ACKNOWLEDGMENT

The research reported in this paper was supported in part by the NASA ARMD/AvSP IVHM project under NRA NNX09AY54A. The support is gratefully acknowledged.

#### REFERENCES

- Bhaumik, S. K., Sujata, M., & Venkataswamy, M. A. (2008) Fatigue failure of aircraft components. *Engineering Failure Analysis*, 15, 675-694.
- Cheng, J., & Li, Q. S. (2009) Reliability analysis of a long span steel arch bridge against wind-induced stability failure during construction. *Journal of Constructional Steel Research*, 65, 552-558.
- Cizelj, L., Mavko, B., & Riesch-Oppermann, H. (1994) Application of first and second order reliability methods in the safety assessment of cracked steam generator tubing. *Nuclear Engineering and Design*, 147, 359-368.
- Corbly, D. M., & Packman, P. F. (1973) On the influence of single and multiple peak overloads on fatigue crack propagation in 7075-T6511 aluminum. *Engineering Fracture Mechanics*, 5, 479-497.
- de Koning AU, v. d. L. H. (1981). Prediction of fatigue crack growth rates under variable loading using a simple crack closure model. Amsterdam: NLR MP 81023U
- Der Kiureghian, A., Zhang, Y., & Li, C.-C. (1994) Inverse reliability problem. *Journal of Engineering Mechanics, ASCE*, 120(5).
- Dowling, N. E. (2007). *Mechanical behavior of materials : engineering methods for deformation, fracture and fatigue*. Upper Saddle River, NJ  
London: Pearson Prentice Hall ;  
Pearson Education.
- Elber, W. (1971). *The significance of fracture crack closure*. Philadelphia.
- Haldar, A., & Mahadevan, S. (2000). *Probability, reliability, and statistical methods in engineering design*. New York ; Chichester [England]: John Wiley.
- Kam, T. Y., Chu, K. H., & Tsai, S. Y. (1998) Fatigue reliability evaluation for composite laminates via a direct numerical integration technique. *International Journal of Solids and Structures*, 35, 1411-1423.
- Koning, A. U. d. (1981). A simple crack closure model for prediction of fatigue crack growth rates under variable-amplitude loading. *Fracture Mechanics: Thirteenth Conference, ASTM STP 743* (pp. 63-85): American Society for Testing and Materials.
- Liao, M., Xu, X., & Yang, Q.-X. (1995) Cumulative fatigue damage dynamic interference statistical model. *International Journal of Fatigue*, 17, 559-566.
- Liu, Y., & Mahadevan, S. (2007) Stochastic fatigue damage modeling under variable amplitude loading. *International Journal of Fatigue*, 29, 1149-1161.
- Liu, Y., & Mahadevan, S. (2009a) Efficient methods for time-dependent fatigue reliability analysis. *AIAA Journal*, 47, 494-504.
- Liu, Y., & Mahadevan, S. (2009b) Probabilistic fatigue life prediction using an equivalent initial flaw size distribution. *International Journal of Fatigue*, 31, 476-487.
- Liu, Y., Mahadevan, S (2009) Efficient methods for time-dependent fatigue reliability analysis. *AIAA Journal*, 47, 494-504.
- Lu, Z., & Liu, Y. (2010) Small time scale fatigue crack growth analysis. *International Journal of Fatigue*, 32, 1306-1321.
- Mikheevskiy, S., & Glinka, G. (2009) Elastic-plastic fatigue crack growth analysis under variable amplitude loading spectra. *International Journal of Fatigue*, 31, 1828-1836.
- Mohanty, J. R., Verma, B. B., & Ray, P. K. (2009) Prediction of fatigue crack growth and residual life using an exponential model: Part II (mode-I overload induced retardation). *International Journal of Fatigue*, 31, 425-432.
- NASA (2000) *Fatigue crack growth computer program NASGRO Version 3.0-Reference manual. JSC-22267B, NASA, Lyndon B. Johnson Space Center, Texas.*
- Newman, J. C. (1981). *A crack closure model for predicting fatigue crack growth under aircraft spectrum loading*. Philadelphia
- Noroozi, A. H., Glinka, G., & Lambert, S. (2007) A study of the stress ratio effects on fatigue crack growth using the unified two-parameter fatigue crack growth driving force. *International Journal of Fatigue*, 29, 1616.
- Noroozi, A. H., Glinka, G., & Lambert, S. (2008) Prediction of fatigue crack growth under constant amplitude loading and a single overload based on elasto-plastic crack tip stresses and strains. *Engineering Fracture Mechanics*, 75, 188-206.
- Pommier, S. (2003) Cyclic plasticity and variable amplitude fatigue. *International Journal of Fatigue*, 25, 983-997.
- Porter, T. R. (1972) Method of analysis and prediction for variable amplitude fatigue crack growth. *Eng. Fract. Mech*, 4, 717-736.
- Rackwitz, R. a. F., B (1978) Structural Reliability Under Combined Random Load Sequences. *Computers & Structures*, 9, 484-494.

Rackwitz, R. a. F., B (June 1976) Note on Discrete Safety Checking When Using Non-Normal Stochastic Models for Basic Variables. *Load Project Working Session, MIT, Cambridge, MA.*

Ray, A. (2000). A state-space model of fatigue crack growth for real-time structural health management. *Digital Avionics Systems Conferences*, Vol. 2 (pp. 6C1/1 - 6C1/8).

Skaggs, T. H., & Barry, D. A. (1996) Assessing uncertainty in subsurface solute transport: efficient first-order reliability methods. *Environmental Software*, 11, 179-184.

Thorndahl, S., & Willems, P. (2008) Probabilistic modelling of overflow, surcharge and flooding in urban drainage using the first-order reliability method and parameterization of local rain series. *Water Research*, 42, 455-466.

Val, D. V., Stewart, M. G., & Melchers, R. E. (1998) Effect of reinforcement corrosion on reliability of highway bridges. *Engineering Structures*, 20, 1010-1019.

Venkateswara Rao, K. T., & Ritchie, R. O. (1988) Mechanisms for the retardation of fatigue cracks following single tensile overloads: behavior in aluminum-lithium alloys. *Acta Metallurgica*, 36, 2849-2862.

Wheeler, O. E. (1972) Spectrum loading and crack growth *J. Basic Eng., Trans. ASME*, 94, 181-186.

Willenborg J, E. R., Wood RA (1971). A Crack Growth Retardation Model Using an Effective Stress Concept. Wright-Patterson Air Force Base, Ohio: Air Force Flight Dynamics Laboratory.

Xiang, Y., & Liu, Y. (2010 (accepted) ) Inverse first-order reliability method for probabilistic fatigue life prediction of composite laminates under multiaxial loading. *ASCE Journal of Aerospace Engineering*.

**Yibing Xiang:** a graduate research assistant in department of civil engineering at Clarkson University. He received his B.S. degree in civil Engineering from Tongji University in China in 2003, and then he worked as a structural engineer in Shanghai Xiandai Arch Design Company. Since 2007, he started his study at Clarkson University and got his M.S. degree in 2009, and continued his PHD degree. His research interests are probabilistic prognosis, reliability analysis, and system reliability.

**Yongming Liu:** an assistant Professor in the department of civil and environmental engineering. His research interests include fatigue and fracture analysis of metals and composite materials, probabilistic methods, computational mechanics, and risk management. He completed his PhD at Vanderbilt University, and obtained his Bachelors' and Masters'

degrees from Tongji University in China. Dr. Liu is a member of ASCE and AIAA and serves on several technical committees on probabilistic methods and advanced materials.